Measurement 161 (2020) 107904

Contents lists available at ScienceDirect

Measurement

journal homepage: www.elsevier.com/locate/measurement

Remaining useful life prediction for Lithium-ion batteries using fractional Brownian motion and Fruit-fly Optimization Algorithm

Haiyang Wang [a], Wanqing Song [a,*], Enrico Zio [b], Aleksey Kudreyko [c], Yujin Zhang [a]

[a] School of Electronic and Electrical Engineering, Shanghai University of Engineering Science, Shanghai, PR China
[b] Energy Department, Politecnico di Milano, Campus Bovisa, Via La Masa 34/3, Milano, MI 20156, Italy
[c] Department of Medical Physics and Informatics, Bashkir State Medical University, Lenina st. 3, Ufa 450008, Russia

ARTICLE INFO

Article history:
Received 31 July 2019
Received in revised form 16 April 2020
Accepted 24 April 2020
Available online 28 April 2020

Keywords:
Remaining useful life
Long-range dependence
Fractional Brownian motion
Hurst exponent
Maximum likelihood estimation
Fruit-fly Optimization Algorithm

ABSTRACT

In this paper, a novel method base on non-Markovian Fractional Brownian Motion (FBM) is proposed for Lithium-ion batteries remaining useful life (RUL) prediction. Firstly, the FBM degradation model is introduced and the Hurst exponent (H) is calculated. Secondly, the parameters of the FBM model are estimated by maximum likelihood estimation (MLE). The Fruit-fly Optimization Algorithm (FOA) is proposed to optimize the H. Then the procedure for RUL prediction is provided. Capacity degradation data of Lithium-ion batteries is selected as prediction case, and the RUL prediction results are given by two real cases of RUL prediction for lithium-ion batteries. The validity of the proposed method is verified by several evaluation criteria.

1. Introduction

Remaining useful life (RUL) prediction of long-life products, such as lithium-ion batteries degradation, has always been an important research direction in reliability analysis and Prognostic and Health Management (PHM) [1]. Accurate RUL prediction of lithium-ion batteries plays an important role in safety, reliability and economics. In the past few decades, various RUL prediction methods of lithium-ion batteries have been proposed [2]. Referring to relevant literature, it is found that RUL prediction methods are divided into the following categories: physical method, experimental method, data-driven method and hybrid method [3]. At present, the first two methods need professional technical support and strict experimental conditions. The methods are more complex, which makes these RUL prediction methods less popularity. Among the latter two methods, data-driven method is the most widely used method in RUL prediction method, because they directly uses degradation data to build prediction models [4].

Specific data-driven methods for RUL prediction of lithium-ion batteries have advantages and disadvantages. Models based on statistical and probabilistic methods have been used for RUL prediction of lithium-ion batteries [5]. Selina et al. [6] proposed a Naive Bayes (NB) model for RUL prediction of batteries under different operating conditions. The method needs data smoothing before modeling [7]. The application of stochastic process model is also popular [8]. Xu et al. [9] studied the influence of the relaxation effect on the degradation law of lithium-ion batteries and proposed a novel RUL prediction method based on Wiener processes. The process has the characteristic of Markov chain but it is difficult to apply it to the non-linear random degradation data [10,11]. Wang et al. [12] proposed a prognostic method to predict the remaining useful life of lithium-ion batteries by the spherical cubature particle filter. The particle filter algorithm has advantages in non-linear and non-Gaussian systems, but it has the problem of particle degeneration and particle shortage caused by resampling [13–15]. Liu et al. [16] and Zhang et al. [17] developed a batteries RUL prediction method based on the Box-Cox transformation. Data-driven methods based on artificial intelligence are popular methods for RUL prediction in recent years [18]. Wu et al. [19] presented an online approach using feed forward neural network (FFNN) and importance sampling (IS) to estimate lithium-ion battery RUL. However, the neural network method often falls into local optimum because of over-training. Liu et al. [20] implemented a flexible and effective on-line training strategy in RVM algorithm to enhance the lithium-ion battery RUL prediction ability. The disadvantage of this algorithm is that it is difficult to implement large-scale training data [21,22]. Khumprom et al. [23] presented the preliminary development of data-driven

* Corresponding author.
E-mail address: swqls@126.com (W. Song).

https://doi.org/10.1016/j.measurement.2020.107904
0263-2241/

prognostic using a Deep Neural Network (DNN) approach to predict the State of Health and the RUL of the lithium-ion battery, but the validation of deep learning model is complex.

There is a general long-range dependence between the degradation data of actual system. Generally speaking, degradation data actually have two forms of dependence, namely long-range dependence (LRD) and short-range dependence (SRD). The former means that the future degradation states depend on the previous degradation data, the latter indicates that the former data has a negative impact on the future [24]. Many actual system degradation models have LRD. Traditional Markovian method is not suitable for describing such degradation processes.

Fractional Brownian Motion (FBM) is a typical continuous non-Markovian stochastic process with stationary and correlative increments, and one of its forms can show LRD. The dependence of FBM model is mainly described by the Hurst exponent (H). According to different ranges of H, the FBM model can be divided into three forms:$0.5 < H < 1$, $0 < H < 0.5$ and $H = 0.5$. The first two forms represent the fractal characteristic of the model, that is LRD and SRD. In particular, the third form of FBM is standard Brownian Motion [25]. Compared with pure stochastic processes, fractal characteristic is more common in practical applications. In fact, FBM model has been widely used in industry, load forecasting and signal processing. For example, due to continuous heat conduction, the temperature drop in the blast furnace tends to show LRD [26]. It is noteworthy that mechanical vibration signals often seem to be SRD but LRD may still exist in the degradation process of rolling bearings [27]. FBM is an effective method to describe LRD, and the value of H used to judge the dependence is the key to the whole model. Usually H is obtained by approximate calculation. This precision is sufficient for judging the dependence. However, because it is also used for calculating the parameters of the FBM model, accurate H is needed to reduce the error of RUL prediction. Therefore, this paper combines Fruit-fly Optimization Algorithm with the existing FBM model to improve the accuracy of lithium-ion batteries RUL prediction.

The rest of the paper is arranged as follows. In Section 2, the FBM degradation model based on non-Markovian characteristic and Hurst exponent calculation is introduced. Section 3 presents the maximum likelihood estimation of the parameters of the FBM model and the optimization of the Hurst exponent with FOA. Section 4 introduces the procedure of RUL prediction. In Section 5, two RUL prediction cases are carried out based on several sets of degradation data of lithium-ion batteries. Finally, the conclusion is summarized in Section 6.

2. Degradation model

W. DAI and C. C. HEYDE [28] studied the related problems of the FBM and introduced the relationship between short-range dependence (SRD) and long-range dependence (LRD), and gave the definition of stochastic differential equation driven by FBM as follows:

$$dX(t) = \mu dt + \sigma B_H(t), \tag{1}$$

where $X(t)$ represents the general process of degradation, μ and σ represent the drift coefficient and diffusion coefficient, respectively. $\{B_H(t), t \geqslant 0\}$ represents the fractional Brownian motion and H is the Hurst exponent. This exponent is also used to judge self-similarity. The range of H is (0, 1). Generally, there are three cases depending on the value of H:

(1) If $0 < H < 0.5$, the process is short-range dependence
(2) If $H = 0.5$, there is no dependence in the process. The best representative process is the standard Brownian Motion (BM).
(3) If $0.5 < H < 1$, the process has a long-range dependence.

This section focuses on non-Markov degradation process. As mentioned above, FBM is a typical zero-mean Gaussian process with a long-range dependence and fractal characteristic when $0.5 < H < 1$. Therefore, the FBM model can describe non-Markov degradation processes. In the literature, Mandelbrot and Van Ness [29] first introduced FBM as follows:

$$B_H(t) = \frac{1}{\Gamma(H+\frac{1}{2})}\left\{\int_{-\infty}^{0}\left[(t-s)^{H-\frac{1}{2}} - (-s)^{H-\frac{1}{2}}\right]dB(s) + \int_{0}^{t}(t-s)^{H-\frac{1}{2}}dB(s)\right\} \tag{2}$$

where $t, s \geqslant 0$, and $\Gamma(x)$ is the Gamma function:

$$\Gamma(x) = \int_{0}^{\infty} t^{x-1}e^{-t}dt \tag{3}$$

In the FBM model, the Hurst exponent determines the covariance of past and future. The covariance function is as follows:

$$C_H(t,s) = E[B_H(t)B_H(s)] = \frac{{\sigma_B}^2}{2}\left(|t|^{2H} + |s|^{2H} - |t-s|^{2H}\right). \tag{4}$$

It can be seen from the above formula that FBM can be transformed into standard BM when $H = 0.5$. In other words, standard BM is only a special form of FBM.

In order to determine whether a given time series has LRD characteristic, the H needs to be calculated. There are many methods to calculate H, which are usually divided into two types: time domain methods and frequency domain methods. Time domain methods usually process time series directly and calculate H by least square fitting. Specific methods include: variance method, absolute value estimation method, curve fitting estimation method, rescaled range analysis method (R/S analysis method). Frequency domain methods estimate the spectral density of the time series in the frequency domain by Fourier transform. Specific methods include: periodic graph method, Wavelet method, etc.

This paper uses the R/S analysis method to calculate H. The reason for choosing this method is that it is a method to evaluate the degree of self-similarity of a time series. Compared with frequency domain algorithm, it is clearly and easy to implement. In addition, if the number of samples is large enough, the effect of R/S analysis will be better. The specific steps of R/S analysis are as follows:

(1) The time series is divided into A sub-intervals, the length of each sub-interval is n and the mean value of each sub-interval is calculated.
(2) The cumulative deviations between each sub-interval are then calculated.
(3) The extreme differences of each sub-interval are also calculated;
(4) The standard deviations of the samples on each sub-interval are calculated.
(5) The mean value of the ratio of range to variance between all sub-intervals is calculated, which is the rescaled range $(R/S)_n$.
(6) When n changes, iterate steps (1) - (5) to achieve different rescaled ranges;
(7) Logarithms of independent variable n and dependent variable $(R/S)_n$ are taken respectively, and the slope fitted by least squares regression is the value of H.

The process of the R/S method calculating H is shown in Fig. 1. We show the curves of the logarithmic variations of independent variable n and dependent variable $(R/S)_n$ in the first figure. Then in the second figure, we use least square regression

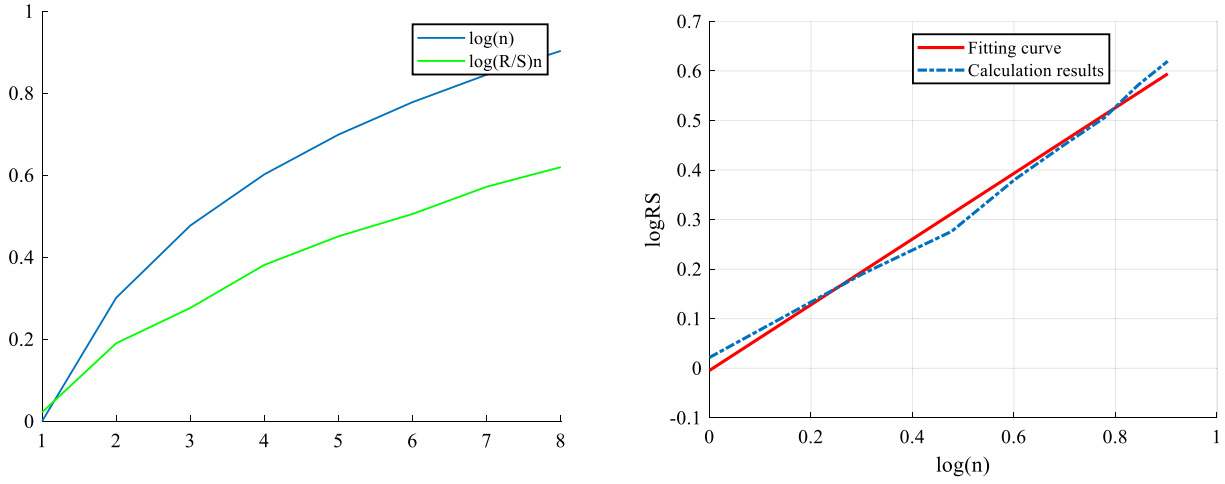

(a) Logarithms of n and $(R/S)_n$ (b) Slope fitted by least squares regression

Fig. 1. Calculation of H by R/S method.

to fit two variables into an approximate straight line, the slope of which is H.

For example, the above R/S method steps applied to the set of available degradation process data of lithium-ion batteries and calculate the value: $H = 0.6401$. The estimated H plays a role in the maximum likelihood estimation of the parameters of the FBM model.

3. Parameters estimation and *H*-optimization

3.1. Parameters estimation

For the FBM model of Eq. (2), we need to estimate the parameters μ and σ. Firstly, the general solution of Eq. (1) can be calculated:

$$\begin{aligned} X(t) &= X_0 \cdot \exp\{-\int -[\mu dt + \sigma dB_H(t)]\} \\ &= X \cdot \exp\left[\int_0^T \mu dt + \sigma dB_H(t)\right] \\ &= X \cdot \exp[\mu t + \sigma B_H(t)] \end{aligned} \tag{5}$$

Taking the logarithmic derivation of Eq. (5):

$$\ln(X(t)) = X(\mu t + \sigma B_H(t)) \tag{6}$$

Therefore, the parameter estimation of Eq. (5) is:

$$Y_t = \mu t + \sigma B_H(t),\ t \geqslant 0 \tag{7}$$

We can assume that the observation interval of the time series is h, for the N observations vector $\mathbf{Y} = (Y_h, Y_{2h}, \ldots, Y_{Nh})'$ and the observation time points $\mathbf{t} = (h, 2h, \ldots, Nh)'$. The FBM model vector is $\mathbf{B}_H(t) = (B_H(h), B_H(2h), \ldots, B_H(Nh))'$. Then, the MLE of parameters μ and σ can be conducted with the following steps [30]:

Step 1: Firstly, according to the joint density function formula of multidimensional normal distribution:

Let the K-dimensional random vector $x = [x_1, x_2, \ldots, x_K]$ obey the multivariate normal distribution with the probability density function:

$$f_{\mu,\Sigma}(x) = f_{\mu,\Sigma}(x_1, x_2, \ldots, x_K) = \frac{1}{(2\pi)^{\frac{K}{2}}} \cdot \frac{1}{|\sum|^{\frac{1}{2}}} \cdot e^{-\frac{1}{2}(x-\mu)^T \sum^{-1}(x-\mu)}, \tag{8}$$

where K is the dimension of the random vector x, and the expected vector μ is also a K-dimensional vector. The covariance matrix is a symmetric positive definite matrix of $K \times K$ dimension:

$$\sum = \begin{bmatrix} \sigma_1^2 & 0 & \ldots & 0 \\ 0 & \sigma_2^2 & \ldots & 0 \\ \ldots & \ldots & \ldots & \ldots \\ 0 & 0 & \ldots & \sigma_K^2 \end{bmatrix}. \tag{9}$$

Because the observation vector $\mathbf{Y}$ also obeys the multivariate normal distribution, we substitute it into Eq. (8). Then, according to Eq. (4), we can deduce the specific expression of each covariance σ_H^2 in the discrete covariance matrix $\sum_H$:

$$\begin{aligned} \sigma_H^2 &= [E[B_H(ih), B_H(jh)]]_{i,j=1,2,\ldots N} \\ &= \frac{\sigma^2}{2} h^{2H} \left(i^{2H} + j^{2H} - |i-j|^{2H}\right)_{i,j=1,2,\ldots N}. \end{aligned} \tag{10}$$

Finally, the joint probability density function of the multidimensional normal distribution of $\mathbf{Y}$ can be expressed as:

$$g(\mathbf{Y}) = (2\pi\sigma^2)^{-\frac{N}{2}} |\Gamma_H|^{-\frac{1}{2}} \exp\left(-\frac{1}{2\sigma^2}(\mathbf{Y}-\mu\mathbf{t})' \Gamma_H^{-1} (\mathbf{Y}-\mu\mathbf{t})\right), \tag{11}$$

where $\Gamma_H = \frac{1}{2} h^{2H} \left(i^{2H} + j^{2H} - |i-j|^{2H}\right)_{i,j=1,2,\ldots,N}$.

Step 2: Next, the logarithmic likelihood function of the joint probability density function is obtained:

$$\begin{aligned} \ln g(\mathbf{Y}) = &-\frac{N}{2}\ln(2\pi\sigma^2) - \frac{1}{2}\ln|\Gamma_H| \\ &- \frac{1}{2\sigma^2}(\mathbf{Y}-\mu\mathbf{t})' \Gamma_H^{-1} (\mathbf{Y}-\mu\mathbf{t}) \end{aligned} \tag{12}$$

Step 3: In Eq. (12), we calculate the partial derivatives of parameters μ and σ^2 respectively and set them equal to zero.

Step 3.1: calculate the partial derivative of parameter μ

$$\begin{aligned} \frac{\partial \ln g(\mathbf{Y})}{\partial \mu} &= \frac{\partial\left(-\frac{N}{2}\ln(2\pi\sigma^2) - \frac{1}{2}\ln|\Gamma_H| - \frac{1}{2\sigma^2}(\mathbf{Y}-\mu\mathbf{t})'\Gamma_H^{-1}(\mathbf{Y}-\mu\mathbf{t})\right)}{\partial\mu} \\ &= \frac{\partial\left(-\frac{1}{2\sigma^2}(\mathbf{Y}-\mu\mathbf{t})'\Gamma_H^{-1}(\mathbf{Y}-\mu\mathbf{t})\right)}{\partial\mu} \\ &= \frac{\partial\left(-\frac{1}{2\sigma^2}\left(\mathbf{Y}'\Gamma_H^{-1}\mathbf{Y} - \mu\mathbf{t}'\Gamma_H^{-1}\mathbf{Y} - \mathbf{Y}'\Gamma_H^{-1}\mu\mathbf{t} + \mu^2\mathbf{t}'\Gamma_H^{-1}\mathbf{t}\right)\right)}{\partial\mu} \\ &= -\frac{\left(-\mathbf{t}'\Gamma_H^{-1}\mathbf{Y} - \mathbf{Y}'\Gamma_H^{-1}\mathbf{t} + 2\mu\mathbf{t}'\Gamma_H^{-1}\mathbf{t}\right)}{2\sigma^2} = 0 \end{aligned}$$

Because $\mathbf{Y}, \mathbf{t}$ are real symmetric matrices:

$$\mathbf{t}'\Gamma_H^{-1}\mathbf{Y} + \mathbf{Y}'\Gamma_H^{-1}\mathbf{t} = (\mathbf{t}'\mathbf{Y} + \mathbf{t}\mathbf{Y}')\Gamma_H^{-1} = 2\mathbf{t}'\Gamma_H^{-1}\mathbf{Y}. \tag{13}$$

So the equation above can be written as $\mu \mathbf{t}' \Gamma_H^{-1} \mathbf{t} = \mathbf{t}' \Gamma_H^{-1} \mathbf{Y}$, and the parameter μ can be expressed as:

$$\mu = \frac{\mathbf{t}' \Gamma_H^{-1} \mathbf{Y}}{\mathbf{t}' \Gamma_H^{-1} \mathbf{t}} \tag{14}$$

The MLE of the drift parameter μ is:

$$\hat{\mu} = \frac{\mathbf{t}' \Gamma_H^{-1} \mathbf{Y}}{\mathbf{t}' \Gamma_H^{-1} \mathbf{t}} \tag{15}$$

Step 3.2: calculate the partial derivative of parameter σ^2

$$\begin{aligned} \frac{\partial \ln g(\mathbf{Y})}{\partial \sigma^2} &= \frac{\partial\left(-\frac{N}{2}\ln(2\pi\sigma^2) - \frac{1}{2}\ln|\Gamma_H| - \frac{1}{2\sigma^2}(\mathbf{Y}-\mu\mathbf{t})'\Gamma_H^{-1}(\mathbf{Y}-\mu\mathbf{t})\right)}{\partial \sigma^2} \\ &= -\frac{N}{2\sigma^2} + \frac{(\mathbf{Y}-\mu\mathbf{t})'\Gamma_H^{-1}(\mathbf{Y}-\mu\mathbf{t})}{2\left(\sigma^2\right)^2} = 0 \end{aligned} \tag{16}$$

Then, the Eq. (15) is bring into Eq. (16) to obtain:

$$\sigma^2 = \frac{1}{N} \frac{\left(\mathbf{Y}' \Gamma_H^{-1} \mathbf{Y}\right)\left(\mathbf{t}' \Gamma_H^{-1} \mathbf{t}\right) - \left(\mathbf{t}' \Gamma_H^{-1} \mathbf{Y}\right)^2}{\mathbf{t}' \Gamma_H^{-1} \mathbf{t}} \tag{17}$$

Similarly, the MLE of σ^2 is:

$$\hat{\sigma}^2 = \frac{1}{N} \frac{\left(\mathbf{Y}' \Gamma_H^{-1} \mathbf{Y}\right)\left(\mathbf{t}' \Gamma_H^{-1} \mathbf{t}\right) - \left(\mathbf{t}' \Gamma_H^{-1} \mathbf{Y}\right)^2}{\mathbf{t}' \Gamma_H^{-1} \mathbf{t}} \tag{18}$$

The diffusion parameter σ is the arithmetic square root of σ^2, so its maximum likelihood estimation is as follows:

$$\hat{\sigma} = \sqrt{\frac{1}{N} \frac{\left(\mathbf{Y}' \Gamma_H^{-1} \mathbf{Y}\right)\left(\mathbf{t}' \Gamma_H^{-1} \mathbf{t}\right) - \left(\mathbf{t}' \Gamma_H^{-1} \mathbf{Y}\right)^2}{\mathbf{t}' \Gamma_H^{-1} \mathbf{t}}} \tag{19}$$

3.2. H-optimization

We have established the FBM model with LRD, the Hurst exponent is calculated by R/S method, and the drift coefficient μ and diffusion coefficient σ in the differential equation are also related to H. The value obtained for H may not be sufficiently accurate, so we need to optimize it. In this paper, Fruit-fly Optimization Algorithm (FOA) is used to optimize H. FOA is a novel global search optimization method. By simulating the unique foraging behavior of fruit-flies in biology and based on the superior olfactory and visual search mechanism of fruit-fly individuals, iterative process is carried out in search space to achieve the results of optimization [31]. Fig. 2 shows the process of global optimization of FOA. Since H plays an important role in the whole RUL prediction model, FOA is used to optimize it to achieve higher accuracy.

The specific steps of FOA for H optimization are as follows:

Step 1: Set the fitness function and the initial data: Set up all the initial data needed by FOA: the size of population: *sizepop*, the range of H and the maximum number of iterations: *maxgen*, and set the RUL prediction value as the fitness function. In this paper, we set the size of population as 50, the maximum number of iterations as 100, and the range of H as (0.5, 1).

Step 2: Initialization: Coding according to the range constraints of H, the location of each fruit-fly is randomly initialized. The equations of location initialization are as follows:

$$x = x_{\min} + (x_{\max} - x_{\min}) * rand, \tag{20}$$

$$y = y_{\min} + (y_{\max} - y_{\min}) * rand. \tag{21}$$

where $x_{\max}$ and $x_{\min}$ are the maximum and minimum of x, $y_{\max}$ and $y_{\min}$ are the maximum and minimum of y.

Step 3: Random search to find the best fruit-fly individuals: Random H calculated from individual position values are substituted into the prediction model to calculate RUL prediction value. The real RUL value of the actual model is the fitness reference value. Select the closest value of RUL prediction value calculated from all the population closer to the actual RUL value and save H corresponding to it, as well as the location of fruit-flies at this time. This value can be used as operational reference for subsequent optimization.

Step 4: Update location optimization: Update the population position, iterate again. The new optimal H is substituted into the calculation of RUL prediction value, which is used to judge the fitness value. The cycle lasts until the termination conditions are met. The optimal value of H can achieve the best prediction result.

The flowchart of FOA to find the optimal H is shown in Fig. 3.

The H refers before and after optimization are given in Table 1, and the drift coefficient and diffusion coefficient are compared with those obtained in Table 1 by using actual lithium-ion batteries data.

4. RUL prediction

The remaining useful life of lithium-ion batteries is defined as the first time that the degradation process exceeds the fault

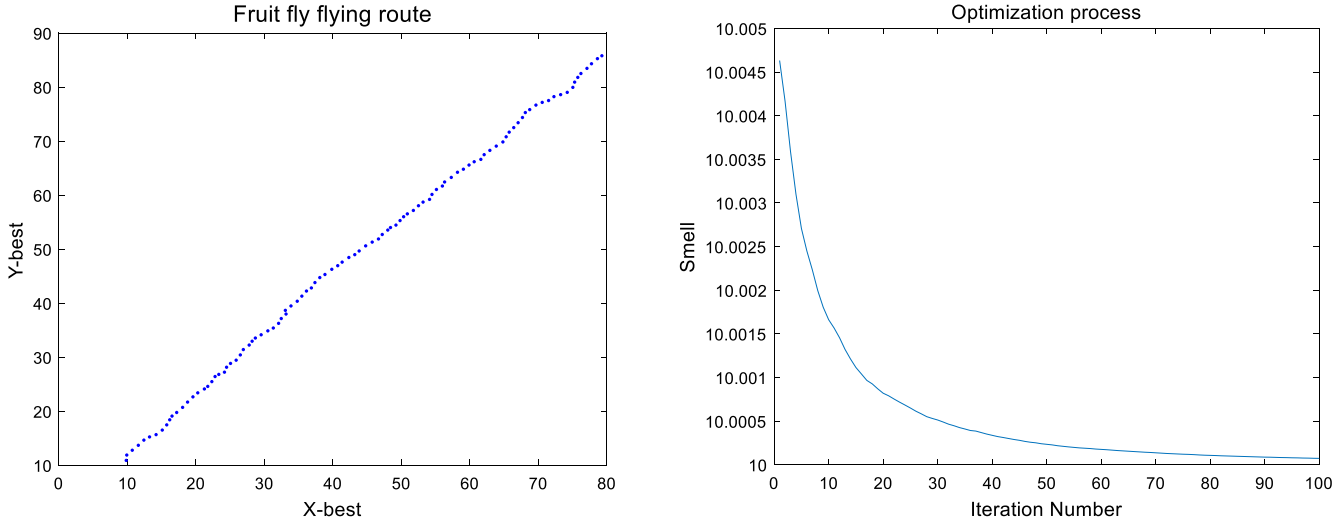

Fig. 2. Optimizing process of FOA.

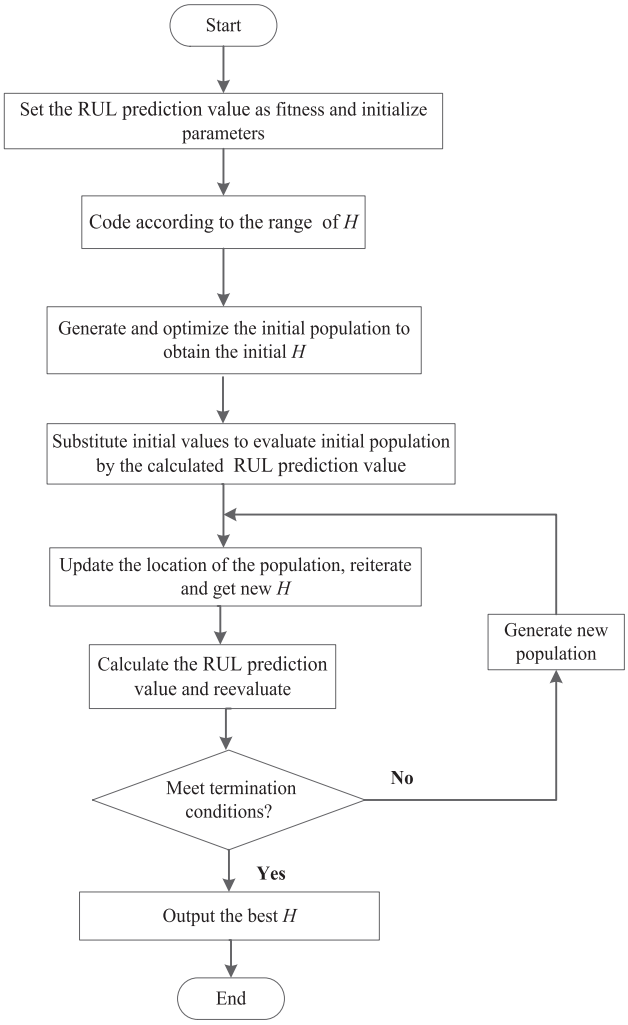

Fig. 3. Flowchart of FOA for finding the optimal H.

Table 1
Comparison of parameters before and after optimization using FOA.

Optimization	H	μ	σ
Before	0.6421	−0.0054	0.0078
After	0.6638	−0.0051	0.0080

threshold. The threshold is based on the regulation of performance test for lithium-ion batteries in international standards. It is considered that when the normal temperature of lithium-ion batteries is 25 ± 2 °C, the lithium-ion batteries will be charged and discharged steadily between 20% and 100% discharging states, until the actual capacity of lithium-ion batteries is reduced to less than 80% of their rated capacity. Batteries that cannot maintain normal operation need to be replaced to ensure the safety and reliability of the normal operation of the system. Therefore, the threshold of the groups of lithium-ion batteries databases in this paper is set to 1.4 Ah (about 70–75% of the rated capacity, due to the difference between different groups of batteries). We set the time which first exceed the threshold as the end-of-life (EOL) point. As shown in Fig. 4. The EOL of lithium-ion battery #05 is equal to 124 cycles and the EOL of lithium-ion battery #06 is equal to 109 cycles.

According to the EOL measured above, the lifetime T can be formally defined as:

$$T = \inf\{t : X(t) \geqslant \omega | X(0) < \omega\}, \tag{22}$$

where the probability density function (PDF) of T can be described as $f_T(t)$(probability density distribution shown in Fig. 2), ω is the preset constant fault threshold level based on performance requirements of different degradation models.

In order to utilize the actual degradation model data for prediction, we set some discrete time points $t_0 < t_1 < t_2 \ldots < t_k$ of the observation of the degradation states and let $x_k = X(t_k)$ represents the observation point of the degenerate model at time t_k. Then a set of observations of the degradation state time points are $\mathbf{X}_0^k = \{x_0, x_1, \ldots, x_k\}$, so according to the concept of EOL, we define RUL L_k at point t_k is:

$$L_k = \inf\{l_k > 0 : X(l_k + t_k) \geqslant \omega\}, \tag{23}$$

The PDF of L_k is $f_{L_k}(l_k)$. The PDF of RUL matching the degradation model with threshold ω is expressed as:

$$\begin{aligned} f_{L_k}(l_k) \cong & \frac{\sigma^{1/2}}{\sqrt{2\pi[\sigma(0)]^{1/2}\int_0^{l_k}[\sigma(h)]^{1/2}dh}} \\ & \times \left\{ \frac{\omega - X(t_k) - \mu l_k}{\int_0^{l_k}[\sigma(h)]^{1/2}dh} + \frac{\mu}{[\sigma(l_k)]^{1/2}} \right\} \\ & \times \exp\left[-\frac{[\omega - X(t_k) - \mu l_k]^2}{2[\sigma(0)]^{1/2}\int_0^{l_k}[\sigma(h)]^{1/2}dh} \right] \end{aligned} \tag{24}$$

where l_k represents the actual RUL, h is the time interval. Based on the definition of $f_{L_k}(l_k)$, it can be seen that it is determined by the drift coefficient μ and diffusion coefficient σ of the degradation process, as well as the fault threshold ω and the system states. The flowchart of the proposed FOA + FBM method is shown in Fig. 5.

In addition, in order to verify the validity of the FBM model for RUL prediction, we compare the predicted results using the parameters of Section 3 calculated by MLE with the numerical results obtained by Monte Carlo simulation method. We select the degradation model data of lithium-ion battery #05 in Fig. 2 above, and validate our simulation prediction results according to the failure threshold set before. Then, we randomly select the starting prediction time point t and predict the final RUL according to the PDF. Using Monte Carlo simulation, the numerical RUL distribution of the LRD model at the same prediction time point is obtained by 1000 simulated sample paths of FBM. As shown in Fig. 6, the predicted results with the estimated parameters can approximately match the RUL distribution obtained by Monte Carlo numerical simulation.

5. Case study

In this section, two cases of actual lithium-ion batteries data are used to apply the proposed FOA + FBM model for RUL prediction. In order to reveal its advantages, the prediction effect of the optimized model is compared with that of the original model in case 1. In case 2, the Relevance Vector Machine (RVM) model, which is a popular data-driven method, is compared with the FOA + FBM model in the prediction of the RUL of lithium-ion batteries.

5.1. Case 1

In case 1, we test the validity of our proposed model using an open source data set of lithium-ion batteries from the NASA Ames prediction database [32]. Capacity represents the amount of remaining energy of lithium-ion batteries, which can be regarded as an important indicator of battery degradation. The experimental data record includes two kinds of time scales: the actual time scale and the cycle time scale. In this paper, the cycle time scale is used. The capacity degradation process of four lithium-ion batteries is

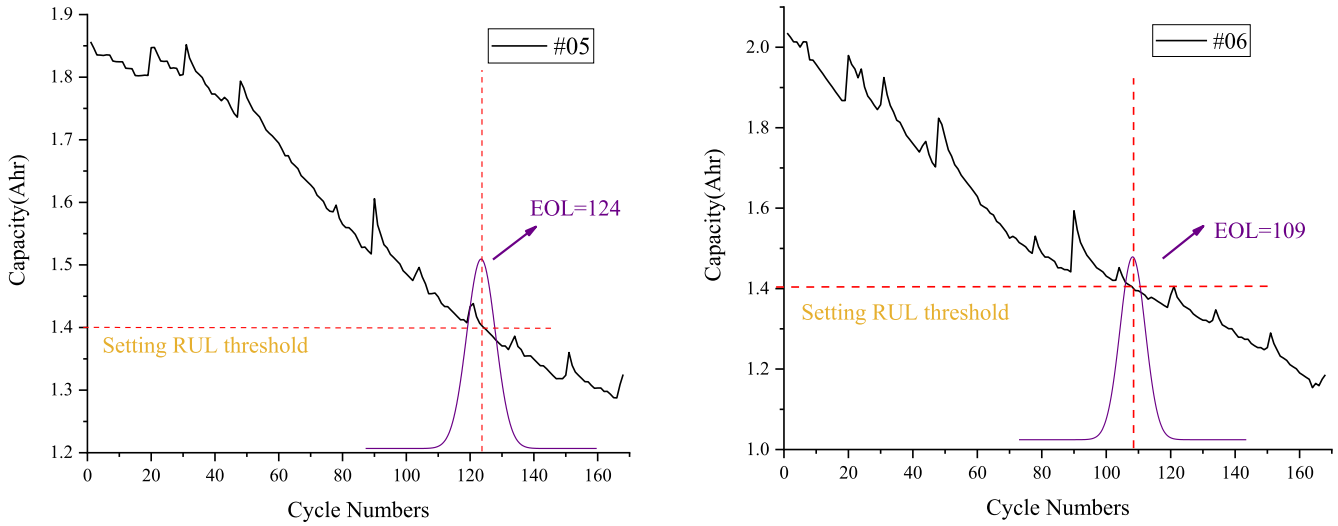

Fig. 4. Process of RUL prediction.

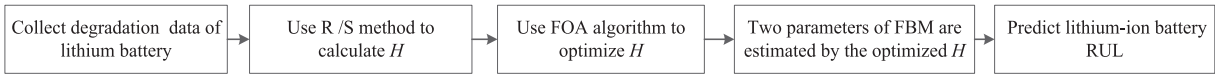

Fig. 5. Flowchart of the proposed FOA + FBM method.

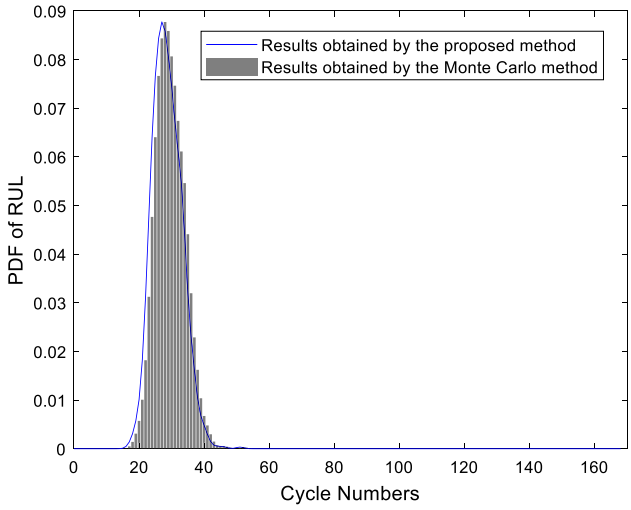

Fig. 6. Comparisons of PDFs obtained by the proposed method and the Monte Carlo method.

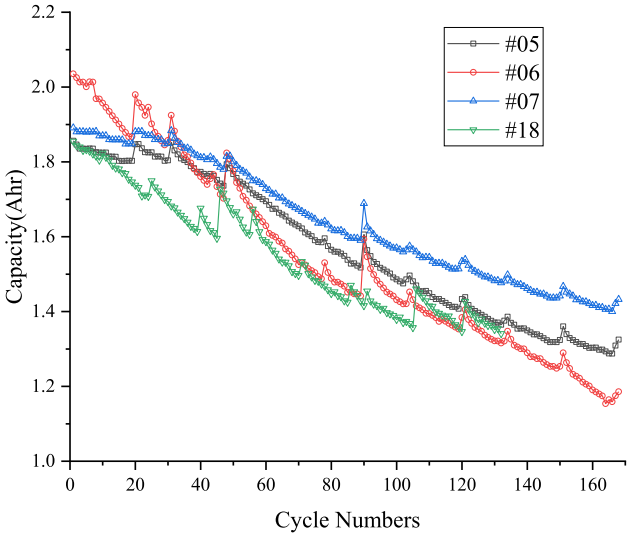

Fig. 7. Lithium-ion batteries degradation model.

shown in Fig. 7, which are #05, #06, #07 and #18, respectively. The failure threshold is set to 1.4 Ah.

The RUL prediction of lithium-ion battery degradation model data is carried out by using the proposed FBM model and the FOA optimized FBM. According to the actual effect of four degradation processes of batteries data, this paper selects two groups of batteries #05 and #06 which are more smooth degradation processes for experimental calculation. The reason why not using the other two groups is that #07 battery degradation process is slower and fails to reach the given failure threshold. While the degradation process of #18 battery degradation process is relatively short, and it is not suitable for experimental prediction. Fig. 8 shows the PDFs comparison for #05 and #06 batteries using the FBM and FOA + FBM. Twelve cycle time points are selected in this experiment, # 05 battery is selected for each of the three cycle intervals, and #06 battery is selected for each cycle interval.

Finally, this paper shows the predicted results of the two groups of lithium-ion batteries from the initial prediction time point in Table 2 and Table 3 respectively. The Relative Error (RE) between the actual RUL and the predicted RUL of each prediction point is calculated as follows:

$$\mathrm{RE} = \frac{\left|RUL_i^f - RUL_i^r\right|}{RUL_i^r} \times 100\% \tag{25}$$

where RUL_i^f represents the RUL between the initial prediction time point i and the predicted EOL, and RUL_i^r represents the RUL between the initial prediction time point i and the actual EOL.

The above two tables and the calculation of Relative Error can only reflect the prediction effect of each prediction point. In order to show the prediction effect of RUL for lithium-ion batteries

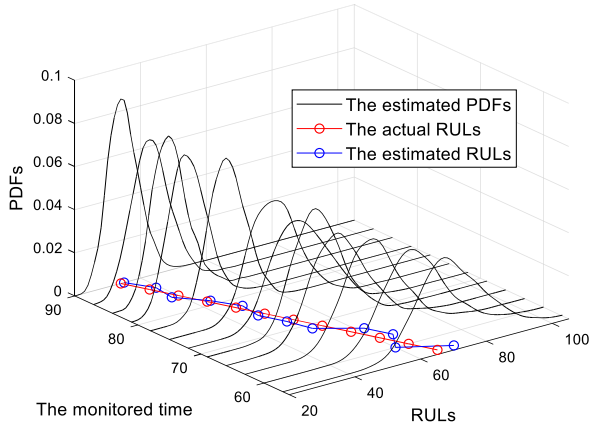

(a) PDF for FBM prediction of #05

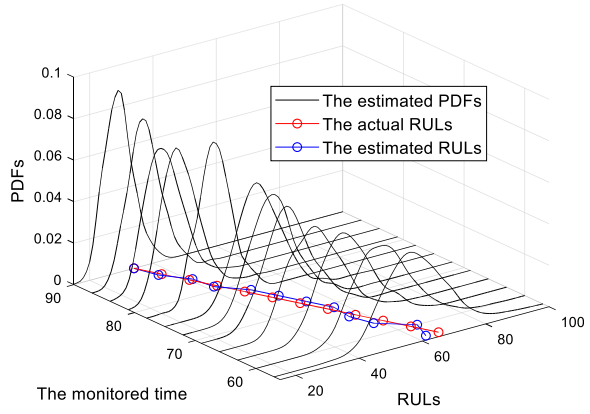

(b) PDF for FBM+FOA prediction of #05

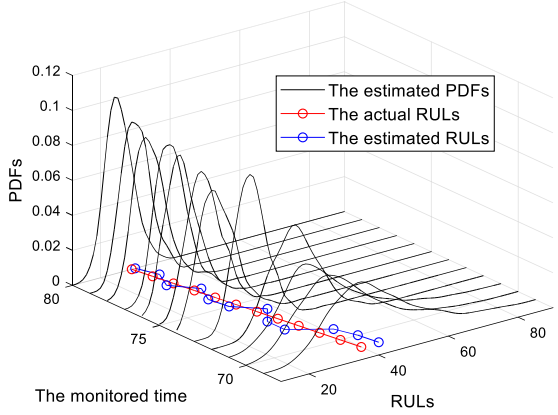

(c) PDF for FBM prediction of #06

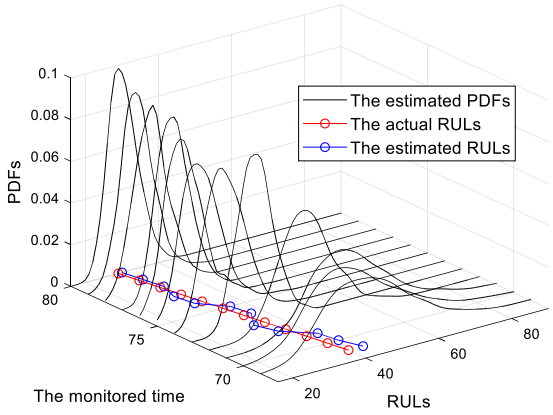

(d) PDF for FBM+FOA prediction of #06

Fig. 8. PDF of RUL predicted by FBM and FOA + FBM for #05, #06.

Table 2
RUL prediction results of #05 lithium-ion battery using FBM and FOA + FBM.

# 05 prediction time point t	Actual RUL	Predicted RUL by FBM	Relative error (%)	Predicted RUL by FOA + FBM	Relative error (%)
57	67	72	7.462	63	5.970
60	64	60	6.250	66	3.125
63	61	65	6.557	58	4.918
66	58	62	6.896	56	3.448
69	55	52	5.454	57	3.636
72	52	50	3.846	54	3.846
75	49	47	4.081	51	4.081
78	46	48	4.347	48	4.347
81	43	44	2.325	42	2.325
84	40	38	5.000	41	2.500
87	37	39	5.405	36	2.702
90	34	35	2.941	34	0

degradation model more intuitively and comprehensively, this paper uses quantitative error indices to evaluate the overall prediction performance: Mean Square Error (MSE) and Root Mean Square Error (RMSE) as follows:

$$\mathrm{MSE} = \frac{1}{N}\sum_{i=1}^{N}\left(RUL_i^f - RUL_i^r\right)^2 \tag{26}$$

$$\mathrm{RMSE} = \sqrt{\frac{1}{N}\sum_{i=1}^{N}\left(RUL_i^f - RUL_i^r\right)^2} \tag{27}$$

where N represents the number of prediction time points. In Table 4, all the parameters of the two prediction methods are listed for comparison. We can see that the FBM model optimized by FOA has higher prediction accuracy for RUL than the original FBM by itself.

5.2. Case 2

In case 2, we select different lithium-ion batteries degradation data and compare with the RVM model. RVM model is based on Markov process and Bayesian analysis theory. RVM

Table 3
RUL prediction results of #06 lithium-ion battery using FBM and FOA + FBM.

# 06 prediction time point t	Actual RUL	Predicted RUL by FBM	Relative error (%)	Predicted RUL by FOA + FBM	Relative error (%)
69	40	45	12.500	44	10.000
70	39	44	12.820	42	7.692
71	38	42	10.526	41	7.894
72	37	33	10.810	35	5.405
73	36	33	8.333	33	8.333
74	35	38	8.571	37	5.714
75	34	32	5.882	36	5.882
76	33	31	6.060	31	6.060
77	32	34	6.250	30	6.250
78	31	29	6.451	32	3.225
79	30	32	6.667	31	3.333
80	29	30	3.448	30	3.448

Table 4
Model parameters and prediction error indices for RUL prediction.

	#05 FBM	#05 FOA + FBM	#06 FBM	#06 FOA + FBM
H	0.6421	0.6638	0.6498	0.6628
μ	−0.0054	−0.0051	−0.0112	−0.0100
σ	0.0078	0.0080	0.0083	0.0089
MSE	8.6667	**4.3333**	10.0835	**5.5000**
RMSE	2.9431	**2.0813**	3.1754	**2.3456**

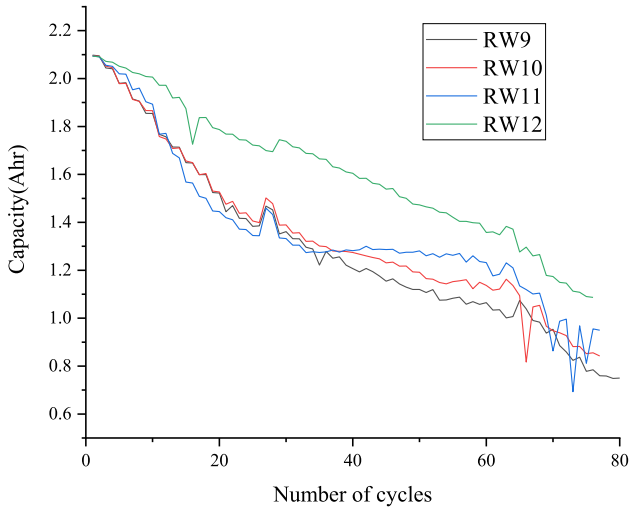

Fig. 9. Random walk lithium-ion batteries degradation model.

uses the calculation of autocorrelation function to judge the prior probability. Because of the advantages of probabilistic prediction, it has been used for the RUL prediction of lithium-ion batteries [33].

The data of lithium-ion batteries in this experiment is the random walk (RW) degraded lithium-ion batteries data set published in 2014 in the open source database of NASA [34]. The capacity degradation process of four lithium-ion batteries (RW9, RW10, RW11, RW12) are shown in Fig. 9 The initial capacity of the degradation process is 2.1 Ah. The failure threshold is also set to 1.4 Ah.

In order to get better prediction results, we use RW12 data, which is more smooth degradation process to predict the RUL of lithium-ion battery. Because the degraded data length of RW batteries capacity is only half of case 1. Therefore, six prediction cycle time points are selected in this comparative experiment, one for every two cycle time intervals. Fig. 10 shows the PDFs comparison of RW12 lithium-ion battery predicted by FOA + FBM and RVM, respectively.

The MSE and RMSE are still used to show the overall prediction effect of the prediction methods. The experimental error results are shown in Table 5.

Table 5
Error evaluation indices of RUL prediction for RW12.

RW12	FOA + FBM	RVM
MSE	**1.2771**	2.9033
RMSE	**1.1301**	1.7039

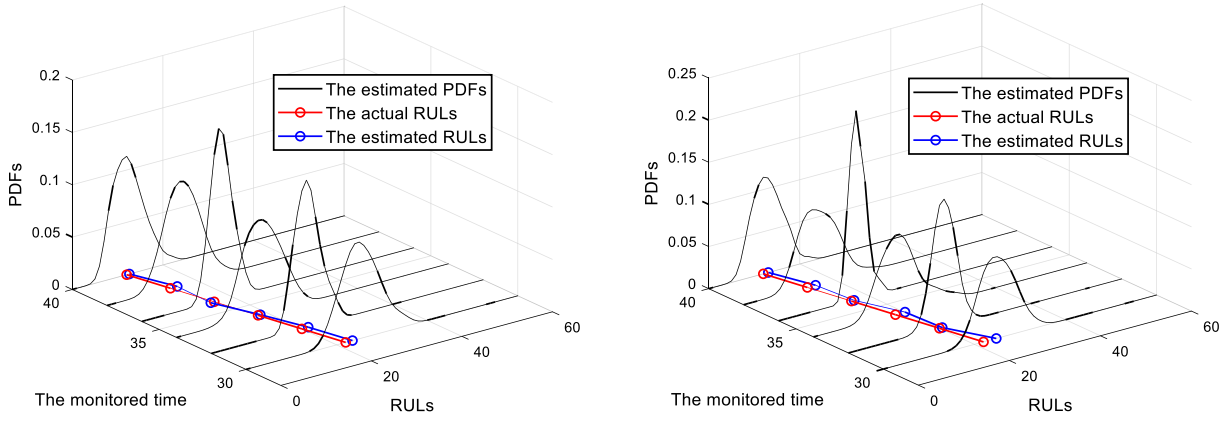

Fig. 10. PDF of RUL predicted by FOA + FBM and RVM for RW12.

6. Conclusion

In this paper, a method of predicting RUL of lithium-ion batteries based on FBM model with LRD is introduced, and the H of the predicted model is optimized by FOA. Firstly, FBM degradation model based on non-Markovian characteristic and H calculation is introduced and the maximum likelihood estimation of drift coefficient μ and diffusion coefficient σ are described. Because of the defect of fitting calculation, this paper puts forward the method of using FOA to optimize H. The prediction process of RUL for lithium-ion batteries degradation data is introduced in detail. The Monte Carlo simulation method is used to compare with the prediction effect of RUL. Finally, through two real cases of RUL prediction for lithium-ion batteries, the FBM model combined with FOA is compared with the original FBM model and RVM model respectively. Combined with the final error evaluation indices, it is proved that the proposed FBM model combined with FOA has better prediction effect. The authors will improve FOA to further improve the prediction accuracy in the future work.

CRediT authorship contribution statement

Haiyang Wang: Conceptualization, Methodology, Software, Investigation, Writing - original draft. **Wanqing Song:** Validation, Formal analysis, Visualization, Software. **Enrico Zio:** Writing - review & editing. **Aleksey Kudreyko:** Writing - review & editing. **Yujin Zhang:** Writing - review & editing.

Declaration of Competing Interest

The authors declare that they have no known competing financial interests or personal relationships that could have appeared to influence the work reported in this paper.

Acknowledgments

This project is supported by Natural Science Foundation of Shanghai (17ZR1411900, 14ZR1418500).

References

[1] D. Wang, K.L. Tsui, Q. Miao, Prognostics and health management: a review of vibration based bearing and gear health indicators, Ieee Access 6 (2018) 12.
[2] P. Khumprom, N. Yodo, A data-driven predictive prognostic model for lithium-ion batteries based on a deep learning algorithm, Energies 12 (4) (2019).
[3] F. Ahmadzadeh, J. Lundberg, Remaining useful life estimation: review, Int. J. System Assurance Eng. Manage. 5 (4) (2014) 461–474.
[4] X. Li, L. Zhang, Z. Wang, Remaining useful life prediction for lithium-ion batteries based on a hybrid model combining the long short-term memory and Elman neural networks, J. Energy Storage 21 (2019) 510–518.
[5] D.T. Liu, W. Xie, H.T. Liao, Y. Peng, An integrated probabilistic approach to lithium-ion battery remaining useful life estimation, Ieee Trans. Instrument. Measur. 64 (3) (2015) 660–670.
[6] Bin Duan, Qi Zhang, Fei Geng, Chenghui Zhang, Remaining useful life prediction of lithium-ion battery based on extended Kalman particle filter, Int. J. Energy Res. 44 (3) (2020) 1724–1734, https://doi.org/10.1002/er.v44.310.1002/er.5002.
[7] H. Liu, W. Song, M. Li, A. Kudreyko, E. Zio, Fractional Lévy stable motion: finite difference iterative forecasting model, Chaos Solitons Fractals 133 (4) (2020) 109632.
[8] F. Li, J.P. Xu, A new prognostics method for state of health estimation of lithium-ion batteries based on a mixture of Gaussian process models and particle filter, Microelectron. Reliab. 55 (7) (2015) 1035–1045.
[9] X.D. Xu, C.Q. Yu, S.J. Tang, X.Y. Sun, X.S. Si, L.F. Wu, Remaining useful life prediction of lithium-ion batteries based on wiener processes with considering the relaxation effect, Energies 12 (9) (May 2019) 17.
[10] W. Qin, H. Lv, C. Liu, D. Nirmalya, P. Jahanshahi, Remaining useful life prediction for lithium-ion batteries using particle filter and artificial neural network, Indust. Manage. Data Syst. 120 (2) (2019) 312–328.
[11] J. Liu, Z.Q. Chen, Remaining useful life prediction of lithium-ion batteries based on health indicator and gaussian process regression model, Ieee Access 7 (2019) 39474–39484.
[12] D. Wang, F.F. Yang, K.L. Tsui, Q. Zhou, S.J. Bae, Remaining useful life prediction of lithium-ion batteries based on spherical cubature particle filter, Ieee Trans. Instrument. Measur. 65 (6) (2016) 1282–1291.
[13] Y.C. Song, D.T. Liu, C. Yang, Y. Peng, Data-driven hybrid remaining useful life estimation approach for spacecraft lithium-ion battery, Microelectron. Reliab. 75 (Aug) (2017) 142–153.
[14] Z.B. Liu, G.Y. Sun, S.H. Bu, J.W. Han, X.J. Tang, M. Pecht, Particle learning framework for estimating the remaining useful life of lithium-ion batteries, Ieee Trans. Instrument. Measur. 66 (2) (2017) 280–293.
[15] X. Zhang, Q. Miao, Z.W. Liu, Remaining useful life prediction of lithium-ion battery using an improved UPF method based on MCMC, Microelectron. Reliab. 75 (Aug) (2017) 288–295.
[16] D.T. Liu, J.B. Zhou, H.T. Liao, Y. Peng, X.Y. Peng, A health indicator extraction and optimization framework for lithium-ion battery degradation modeling and prognostics, Ieee Trans. Syst. Man Cybernet.-Syst. 45 (6) (2015) 915–928.
[17] Y.Z. Zhang, R. Xiong, H.W. He, M.G. Pecht, Lithium-ion battery remaining useful life prediction with box-cox transformation and Monte Carlo simulation, Ieee Trans. Indust. Electron. 66 (2) (2019) 1585–1597.
[18] X.Y. Li, L. Zhang, Z.P. Wang, P. Dong, Remaining useful life prediction for lithium-ion batteries based on a hybrid model combining the long short-term memory and Elman neural networks, J. Energy Storage 21 (Feb) (2019) 510–518.
[19] J. Wu, C.B. Zhang, Z.H. Chen, An online method for lithium-ion battery remaining useful life estimation using importance sampling and neural networks, Appl. Energy 173 (2016) 134–140.
[20] D.T. Liu, J.B. Zhou, D.W. Pan, Y. Peng, X.Y. Peng, Lithium-ion battery remaining useful life estimation with an optimized Relevance Vector Machine algorithm with incremental learning, Measurement 63 (Mar) (2015) 143–151.
[21] W.Q. Song, X.X. Chen, C. Cattani, MultiFractional Brownian motion and quantum-behaved partial swarm optimization for bearing degradation forecastin, Complexity, 2020, https://doi.org/10.1155/2020/8543131.
[22] M.A. Patil, P. Tagade, K.S. Hariharan, S.M. Kolake, T. Song, T. Yeo, S. Doo, A novel multistage Support Vector Machine based approach for Li ion battery remaining useful life estimation, Appl. Energy 159 (Dec) (2015) 285–297.
[23] P. Khumprom, N. Yodo, A data-driven predictive prognostic model for lithium-ion batteries based on a deep learning algorithm, Energies 12 (4) (2019) 21.
[24] Xiaopeng Xi, Maoyin Chen, Hanwen Zhang, Donghua Zhou, An improved non-Markovian degradation model with long-term dependency and item-to-item uncertainty, Mech. Syst. Signal Process. 105 (2018) 467–480, https://doi.org/10.1016/j.ymssp.2017.12.017.
[25] Z.-X. Zhang, X.-S. Si, C.-H. Hu, An age- and state-dependent nonlinear prognostic model for degrading systems, Ieee Trans. Reliab. 64 (4) (2015) 1214–1228.
[26] H. Zhang, M. Chen, X. Xi, D. Zhou, Remaining useful life prediction for degradation processes with long-range dependence, IEEE Trans. Reliab. 66 (4) (2017) 1368–1379.
[27] Y.D. Gao, V. Francesco, L. Ming, et al., Multi-scale permutation entropy based on improved LMD and HMM for rolling bearing diagnosis, Entropy 19 (4) (2017) pp. 176-.
[28] C.C. Heyde, W. Dai, Ito's formula with respect to fractional Brownian motion and its application, J. Appl. Math. Stochastic Anal. 4 (1996) 439–448.
[29] B.B. Mandelbrot, Fractional Brownian motions, fractional noises and applications, SIAM Rev. 10 (4) (1968) 422–437.
[30] W.Q. Song, C. Cattani, C.H. Chi, Multifractional Brownian motion and quantum-behaved particle swarm optimization for short term power load forecasting. An integrated approach, Energy 194 (1) (2020) 116847.
[31] W.-T. Pan, A new Fruit Fly Optimization Algorithm: taking the financial distress model as an example, Knowledge-Based Syst. 26 (Feb) (2012) 69–74.
[32] B. Saha, K. Goebel, Battery Data Set, NASA Ames Prognostics Data Repository, 2007. http://ti.arc.nasa.gov/project/prognostic-data-repository.
[33] X.L. Qin, Q. Zhao, H.B. Zhao, W.Q. Feng, X.M. Guan, Ieee, Prognostics of remaining useful life for lithium-ion batteries based on a feature vector selection and relevance vector machine approach, in: 2017 Ieee International Conference on Prognostics and Health Management (Icphm), 2017, pp. 1–6.
[34] B. Brian, K. Chetan, D. Matthew, Adaptation of an electrochemistry-based li-ion battery model to account for deterioration observed under randomized use, in: The Proceedings of the Annual Conference of the Prognostics and Health Management Society, 2014.